



## INVITED REVIEW

# Use of advanced neuroimaging and artificial intelligence in meningiomas

Norbert Galldiks<sup>1,2,3</sup>  | Frank Angenstein<sup>4,5,6</sup> | Jan-Michael Werner<sup>1</sup> | Elena K. Bauer<sup>1</sup> | Robin Gutsche<sup>2</sup> | Gereon R. Fink<sup>1,2</sup> | Karl-Josef Langen<sup>2,3,7</sup> | Philipp Lohmann<sup>2,8</sup> 

<sup>1</sup>Department of Neurology, Faculty of Medicine, University Hospital Cologne, University of Cologne, Cologne, Germany

<sup>2</sup>Institute of Neuroscience and Medicine (INM-3, -4), Research Center Juelich, Juelich, Germany

<sup>3</sup>Center for Integrated Oncology (CIO), Universities of Aachen, Cologne, Germany

<sup>4</sup>Functional Neuroimaging Group, Deutsches Zentrum für Neurodegenerative Erkrankungen (DZNE), Magdeburg, Germany

<sup>5</sup>Leibniz Institute for Neurobiology (LIN), Magdeburg, Germany

<sup>6</sup>Medical Faculty, Otto von Guericke University, Magdeburg, Germany

<sup>7</sup>Department of Nuclear Medicine, University Hospital Aachen, Aachen, Germany

<sup>8</sup>Department of Stereotaxy and Functional Neurosurgery, Faculty of Medicine, University Hospital Cologne, University of Cologne, Cologne, Germany

## Correspondence

Norbert Galldiks, Institute of Neuroscience and Medicine (INM-3), Research Center Juelich, Leo-Brandt-St., Juelich 52425, Germany.  
Email: n.galldiks@fz-juelich.de; norbert.galldiks@uk-koeln.de

## Funding information

Supported by the Deutsche Forschungsgemeinschaft (DFG), project number 428090865 (N.G., E.K.B., R.G., P.L.), and the Cologne Clinician Scientist Program (CCSP) / Faculty of Medicine / University of Cologne, funded by the DFG, FI 773/15-1 (J.-M. W.)

## Abstract

Anatomical cross-sectional imaging methods such as contrast-enhanced MRI and CT are the standard for the delineation, treatment planning, and follow-up of patients with meningioma. Besides, advanced neuroimaging is increasingly used to non-invasively provide detailed insights into the molecular and metabolic features of meningiomas. These techniques are usually based on MRI, e.g., perfusion-weighted imaging, diffusion-weighted imaging, MR spectroscopy, and positron emission tomography. Furthermore, artificial intelligence methods such as radiomics offer the potential to extract quantitative imaging features from routinely acquired anatomical MRI and CT scans and advanced imaging techniques. This allows the linking of imaging phenotypes to meningioma characteristics, e.g., the molecular-genetic profile. Here, we review several diagnostic applications and future directions of these advanced neuroimaging techniques, including radiomics in preclinical models and patients with meningioma.

## KEY WORDS

MRI, PET, radiogenomics, radiomics

## 1 | INTRODUCTION

The most frequently reported histology of all primary brain and other central nervous system tumors is

meningioma and comprises 37.6% with an average annual incidence rate of 8.58 patients per 100,000 population [1].

Contrast-enhanced structural magnetic resonance imaging (MRI) is routinely used in meningioma patients

This is an open access article under the terms of the Creative Commons Attribution License, which permits use, distribution and reproduction in any medium, provided the original work is properly cited.

© 2021 The Authors. *Brain Pathology* published by John Wiley & Sons Ltd on behalf of International Society of Neuropathology

for defining the tumor extent, treatment planning, and follow-up after treatment, especially for the diagnosis of tumor recurrence. Additionally, computed tomography (CT) allows, besides identifying calcifications for differential diagnosis, the diagnosis of osseous involvement of the adjacent skull bone [2, 3], which is of particular value for meningioma delineation and treatment-decisions. While structural MRI is exceptional in providing information on both the central nervous system anatomy and meningiomas, advanced neuroimaging techniques offer the ability to yield additional information regarding tumor biology at both the functional and molecular levels. In neurooncology, these techniques are usually based on MRI, e.g., perfusion-weighted imaging (PWI), diffusion-weighted imaging (DWI), MR spectroscopy (MRS), and positron emission tomography (PET).

Moreover, artificial intelligence offers the potential to extract additional imaging features from routinely acquired MRI, CT, and advanced imaging techniques. Importantly, these features quantify image characteristics that are beyond human perception. In combination with clinical parameters or molecular markers, mathematical or machine learning models can be developed for an improved assessment of prognosis or the non-invasive prediction of molecular-genetic alterations. The development of these models based on quantitative features computed from medical images is called radiomics [4–7] and allows linking imaging phenotypes to a tumor's molecular-genetic profile, a field commonly referred to as radiogenomics. The latter is also of particular interest because efforts are currently ongoing to incorporate molecular profiling into the diagnostic work-up to improve the characterization of meningiomas, e.g., in terms of prediction of the biological behavior [8].

Furthermore, deep learning-based radiomics uses artificial neural networks that automatically extract high-dimensional features from the images at different abstraction levels. As a result, characteristic image patterns are autonomously identified, learned, and used for classification [9].

Here, we review several diagnostic applications and future directions of these advanced neuroimaging techniques, including radiomics in preclinical models and patients with meningioma.

## 2 | NEUROIMAGING OF PRECLINICAL MENINGIOMA MODELS

Various meningioma animal models were successfully established during the last years to study the mechanisms of tumor initiation and progression and the efficacy and toxicity of novel treatment approaches [10, 11]. Ideally, not only the presence and exact location of the tumor growth can be visualized, but also the rate of tumor growth can be quantified in longitudinal

measurements before or after treatment. Thus, slowing down tumor growth or even tumor regression following treatment may become detectable in individual animals. An essential prerequisite for such longitudinal tumor imaging is a non-invasive nature of the imaging modality that allows examinations of even weakened animals (e.g., due to treatment side effects). Currently, mice are mainly used as animal models, and therefore imaging modalities with a high spatial resolution are required to depict a meningioma as a total nude mouse brain has only a volume of about 450 mm<sup>3</sup>. Additionally, to detect pathological relevant changes in meningioma growth, imaging with submillimeter range resolution is crucial to evaluate putative cancer treatment effects.

There are basically two options to distinguish the meningioma from surrounding healthy tissue under in vivo conditions. First, already existing structural changes related to the tumor growth can be visualized. Second, tumor cells can be labeled either intrinsically (i.e., tumor cells express a detectable marker) or extrinsically (i.e., an external applied detectable marker specifically binds to tumor cells). Besides others, frequently used non-invasive imaging modalities are bioluminescence imaging, MRI, and PET.

### 2.1 | Bioluminescence imaging

The labeling of tumor cells with an easily detectable marker, such as different luciferases (i.e., firefly luciferase, marine *Renilla* luciferase, or *Oplophorus* luciferase), is an intriguing approach to identify the location and putative spreading of the meningioma over time in individual animals [12]. Because luciferase expression is cell-specific, the bioluminescence signal indicates the presence and location of meningioma cells. An augmented signal intensity relates to an increased number of cells that express the respective marker and thus indicates tumor growth. Besides, bioluminescence provides information on tumor cell viability. Luciferases only produce light in the presence of the substrates luciferin or coelenterazine, which have to be applied before imaging, and of intracellular adenosine triphosphate, oxygen, and Mg<sup>2+</sup>. Thus, light is only generated in living cells [13, 14]. This also means that dead tumor cells, infiltrating host cells, and tumor cell debris do not contribute to the bioluminescence signal [15]. Thus, the total tumor size does not necessarily relate to the measured bioluminescence signal. Nevertheless, one should keep in mind that artificial expression of luciferase may itself affect the immune response toward these cells, which may eventually result in reduced growth of these reporter-labeled cells [16–18].

So far, human immortal IOMM-Lee cells (intraosseous malignant meningioma-derived cell line) were transfected with firefly luciferase. As early as 3 days after implantation at the skull base, bioluminescence

imaging successfully detected the tumor, and, subsequently, signals increased nearly exponentially until day 18 [19]. Although imaging was highly sensitive, the exact location and extent of the meningioma had to be verified by subsequent histological analysis. In a similar study, another human immortal cell line (CH-157-MN), as well as IOMM-Lee cells, was implanted at the skull base or at the cerebral convexity of 3-week-old immunodeficient mice. Bioluminescence signals were measured biweekly starting 1 week after implantation [20]. According to the measured bioluminescence signals, almost logarithmic tumor growth was detected until day 17–18.

In addition to human immortal cell lines, mouse neonatal arachnoidal cells with inactivated *Nf2* and *Cdkn2ab* genes were injected at the craniocervical junction in immunocompetent 6-week-old mice. These cells, which were also co-transfected with a luciferase reporter gene, developed to higher-grade meningioma. In these mice, bioluminescence imaging could detect growing tumors at the skull base or convexity of 3-month-old mice [21].

In general, bioluminescence imaging provides an improved approximation of the actual tumor burden, but only limited information about the tumor's exact spatial distribution. Therefore, it has to be considered to transfect meningioma tumor cells with a secreted luciferase and, for tumor growth monitoring, a corresponding blood luciferase reporter gene assay is necessary [22].

This approach is an inexpensive, rapid, nevertheless it is a sensitive method to measure tumor growth and response to various treatments.

## 2.2 | Magnetic resonance imaging

So far, MRI has the highest spatial resolution (up to  $25\ \mu\text{m}^2$  in-plane) for soft tissue in vivo imaging. Therefore, several anatomical MRI studies were performed to delineate and quantify the volume of meningiomas. The first study was published in 2003 using a 1.5 T clinical MRI system. In that study, xenografts containing IOMM-Lee cells were implanted at the skull base of mice. T1-weighted MRI could detect the developing tumor after 14 days. These images already had an in-plane resolution of about  $100 \times 100\ \mu\text{m}$ , but a slice thickness of 1.5 mm hampered an accurate volume determination [23]. With the advent of ultra-high field MRI animal systems, spatial resolution increased considerably. The use of 9.4 T animal scanners combined with cryo-coils allows scanning with an in-plane spatial resolution of  $50 \times 50\ \mu\text{m}$ , and a slice thickness of 250  $\mu\text{m}$ .

In most cases, T2-weighted images were sufficient to distinguish the meningioma from the surrounding normal brain tissue (Figure 1). Up to now, various xeno- and allografts were visualized and quantified by anatomical MRI. For example, the impact of micro-RNA 145 on

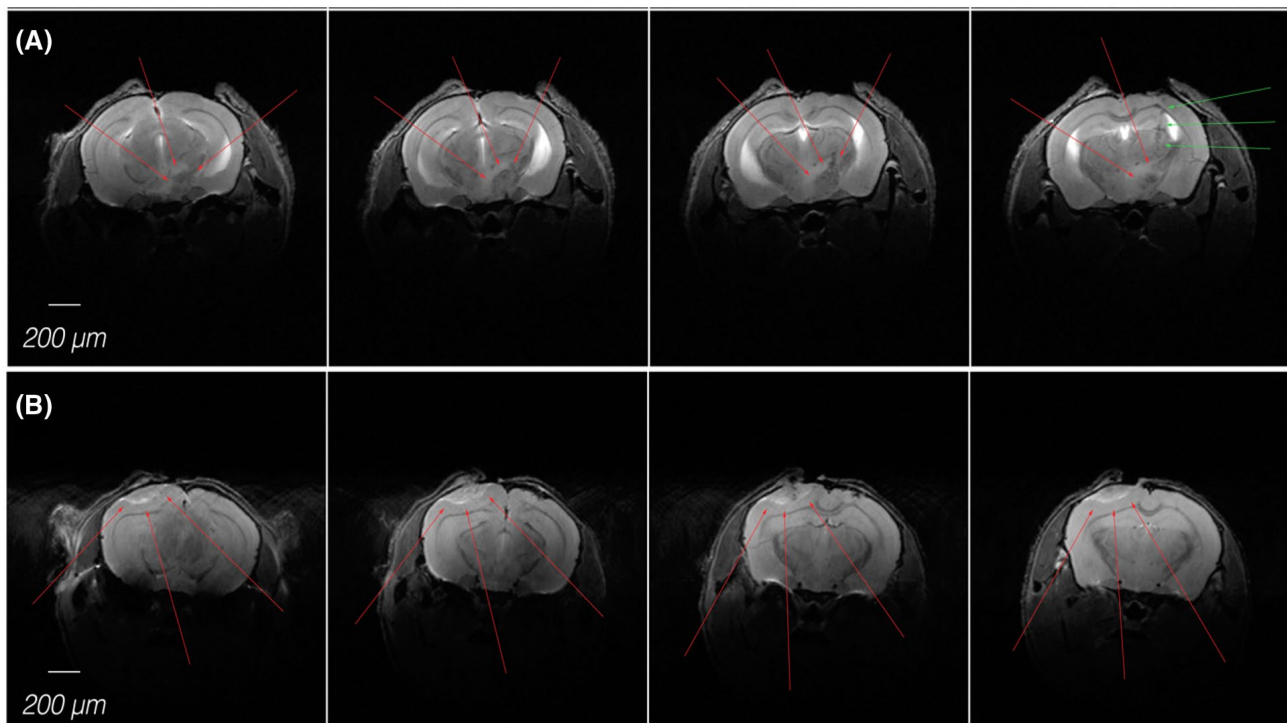


**FIGURE 1** T2-weighted anatomical MR images visualize the location and size of a meningioma either at skull base (A) or at the cerebral convexity (B) of the mouse brain. In-plane resolution of  $52 \times 52\ \mu\text{m}$  (field of view,  $20 \times 20\ \text{mm}$ ; imaging matrix,  $384 \times 384$ ) allows for a clear separation of the meningioma (red arrows) from the surrounding tissue. Green arrows indicate the site for implanting the meningioma cells

IOMM-Lee cell growth at the cortical curvature was determined by T2-weighted MRI [24]. Similarly, an inhibitory effect of temsirolimus, regorafenib, and sorafenib on IOMM-Lee cells growth at the cortical curvature could be verified by serial T2-weighted measurements [25, 26]. Furthermore, the growth of KLF4K40Q transfected IOMM-Lee cells at the convexity and skull base could also be followed and quantified by T2-weighted MRI [27]. A similar imaging approach was also used to follow the slowly growing KT21 meningioma cells at the convexity [28].

In meningiomas, the contrast in T1-weighted images is increased by the intravenous application of a gadolinium-based contrast agent (Figure 2). Corresponding histology confirmed widespread vascularization and, often, hemorrhage in the tumor [29]. In combination with bioluminescence imaging at the craniocervical junction, contrast-enhanced MRI visualized meningioma developed from mouse neonatal arachnoidal cells with an inactivated *Nf2* as well as *Cdkn2ab* gene [21]. Besides detecting xeno- or allografts, contrast-enhanced T1-weighted MRI allows exposing abnormal meningeal proliferations in mice deficient in *Nf2* and *p16* [30]. These spontaneously developing meningiomas were subsequently verified by histology.

In summary, high-resolution MRI is well suited to localize and quantify meningiomas that develop from various cell lines (Figure 3). The main advantage of high-resolution MRI is the possibility to precisely delineate the tumor and visualize possible invasions in bone or even perforations through the skull base. Notably, a combination of different modalities may also increase the informative value. All imaging methods mentioned here can be used for longitudinal studies. In parallel, they can be used to localize and quantify the tumor size, e.g., MRI, or verify tumor cell viability, e.g., bioluminescence imaging. On the other hand, infrastructure and running costs for MRI are more extensive and expensive than bioluminescence imaging. Nevertheless, MRI offers the possibility to perform different imaging sequences (e.g., T1 with or without contrast agent, T2) during one imaging session. Furthermore, current developments in MRI nanoimaging agents, which are highly versatile for on-demand covalent conjugation of various moieties, including proteins [31], may further increase the contrast for meningioma in MR images.

### 2.3 | Positron emission tomography

Meningioma cells are known to highly express somatostatin receptors (SSTR), predominantly the SSTR subtype 2 [32]. Consequently, somatostatin receptor ligands, such as  $^{68}\text{Ga}$ -DOTA-Tyr3-octreotide (DOTATOC),  $^{68}\text{Ga}$ -DOTA-I-Nal3-octreotide (DOTANOC), or  $^{68}\text{Ga}$ -DOTA-D-Phe1-Tyr3-octreotate (DOTATATE) that have high affinity to the SSTR2, were labeled with the

positron-emitting nuclide  $^{68}\text{Ga}$  and used to define the meningioma extent, particularly for treatment planning in patients with meningioma [33].

Currently, the number of animal studies in mice that use SSTR PET ligands is small. Soto-Montenegro and colleagues evaluated a subcutaneous human meningioma CH-157MN xenograft using the latter mentioned  $^{68}\text{Ga}$ -labeled SSTR analogs. Of these,  $^{68}\text{Ga}$ -DOTATATE had the best tumor-to-muscle uptake ratio, indicating that this tracer seems to be the best option for detecting meningiomas [34].

A further DOTATATE PET study evaluated subcutaneously implanted human CH-157MN meningioma xenografts serially after inoculation. On day 20, the DOTATATE PET scan revealed a reduced tumoral tracer binding compared with earlier scans at days 7 and 13, assuming that this reflects necrotic areas within the tumor [35]. Although it has undisputable potential for research applications, PET studies using SSTR ligands have limitations, particularly for mouse imaging. First, the spatial resolution of preclinical PET is inherently limited by physical principles and usually in the range of 0.7–1 mm. Second, signal detection in tiny regions can be easily contaminated by surrounding regions, hampering tracer binding quantification. Third, the use of SSTR PET to quantify tumor growth over time requires a stable expression of somatostatin receptors during early and late stages.

## 3 | USE OF ADVANCED MRI AND PET IN PATIENTS WITH MENINGIOMA

Contrast-enhanced anatomical MRI is exceptional in providing detailed structural information of the central nervous system anatomy and brain neoplasms, although its specificity is comparatively poor [36–40]. Advanced MR techniques, including PWI techniques such as dynamic contrast-enhanced (DCE) or dynamic susceptibility contrast (DSC) PWI and arterial spin labeling (ASL), apparent diffusion coefficients (ADC) obtained by DWI, and proton MRS [41–43], yield additional information regarding tumor biology, especially at the molecular, physiological, and functional levels.

PWI is a non-invasive MRI technique to measure blood flow quantitatively. In Neuro-Oncology, the parameter relative cerebral blood volume is frequently assessed. Most commonly, a gadolinium-based contrast agent is used to assess tissue perfusion. DSC MRI uses the passage of the contrast agent to cause local magnetic field distortion (susceptibility effect) in the vicinity of the vessels resulting in a signal drop in T2- or T2\*-weighted MRI. DCE MRI is based on shortening of the T1-relaxation time causing a signal increase in T1-weighted MRI. ASL is another PWI method which does not require a contrast agent. Here, endogenous water

**FIGURE 2** Meningiomas (red arrows) at the cerebral convexity of the mouse brain delineated using T2-weighted MRI (A) and a subsequently obtained T1-weighted MRI after intravenous application of a gadolinium-based contrast agent (B)

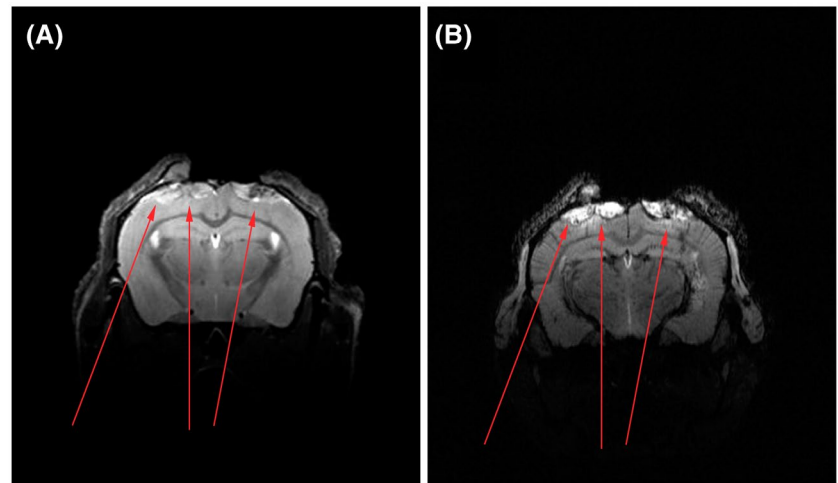
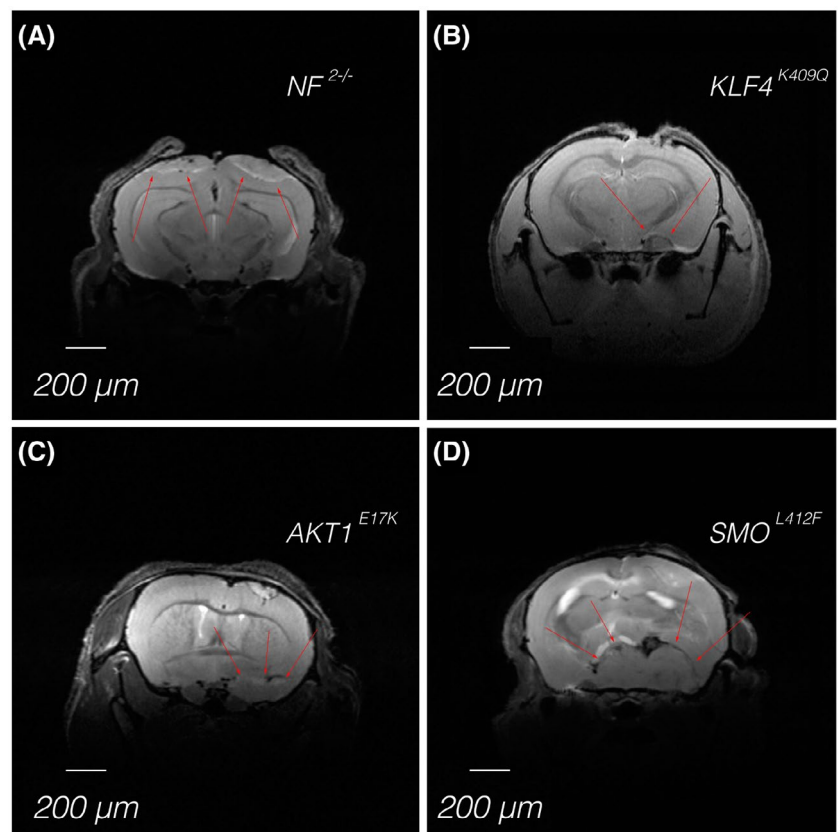


**FIGURE 3** High-resolution MR imaging of meningioma in Swiss nude mice derived from different cell lines carrying either deletion of *NF2* (A) or a mutation in *AKT1* (B), *KLF4* (C), or *SMO* (D). Red arrows indicate the location of the meningiomas



molecules in blood vessels are magnetically labeled by applying a specific radiofrequency pulse. Passage of these labeled molecules through the tissue of interest leads to a reduction of signal intensity in proportion to the perfusion.

DWI is based on the measurement of Brownian motion of water molecules to generate an image contrast. DWI contrast uses two opposing gradient pulses; the first one induces a phase shift in water molecules, leading to a signal reduction. Subsequently, a second opposed

gradient pulse is applied, which rephases the water molecules in the region of interest, leading to a recovery of the water signal.

Proton MRS is a non-invasive method to detect selected water-soluble metabolites in vivo. By the application of external magnetic fields, every metabolite has its characteristic magnetic field signature resulting in slightly different resonance frequencies with differential signals. These signal differences are used in MRS to identify the metabolites of interest.

## 4 | MOST RELEVANT CLINICAL APPLICATIONS FOR ADVANCED MRI

### 4.1 | Differential diagnosis

A wide variety of neoplastic and inflammatory diseases have a propensity for the dura mater or subdural space's involvement and may mimic meningioma. For example, dural-based brain metastases, lymphomas, tumors of the solitary fibrous tumor spectrum (previously referred to as hemangiopericytomas) (Figure 4), as well as sarcoidosis and tuberculosis, may exhibit a meningioma-like appearance [44, 45]. Furthermore, depending on the meningioma size, the distinction between an intraaxial and extraaxial origin may be difficult [46].

Perfusion MRI may differentiate between meningioma and dural metastases from different entities, especially breast cancer and colorectal carcinoma [47]. The cerebral blood volume in these brain metastases entities seems to be significantly lower than in meningiomas. By contrast, brain metastases from renal cell carcinoma or melanoma may also have elevated blood volumes, thereby hampering differential diagnosis of meningioma [48–50]. Using proton MRS, metabolic profile characterization may add valuable information for

the differentiation between meningiomas and brain metastases [51, 52]. A considerable number of meningiomas exhibit a relatively high choline peak at 3.2 parts per million and an inverted doublet alanin peak centered at 1.45 parts per million [52, 53].

### 4.2 | Meningioma grading

In patients with newly diagnosed meningioma, various imaging features derived from preoperative anatomical MRI (e.g., heterogenous contrast enhancement, perifocal edema, presence of a brain–tumor interface) may be associated with an atypical meningioma of the WHO grade II or a WHO grade III anaplastic meningioma [54]. Furthermore, perfusion MRI metrics seem to be of value to differentiate between WHO grade I and grade II or III meningioma. A study suggested that the cerebral blood volume accurately reflects vascular endothelial growth receptor expression and tumor grade in meningiomas and helps identify patients with WHO grade II or III meningioma [55]. Another study observed that perfusion patterns in cerebral blood flow maps derived from ASL are also of value for meningioma grading [56]. In that study, a heterogenous hyperperfusion or a lack

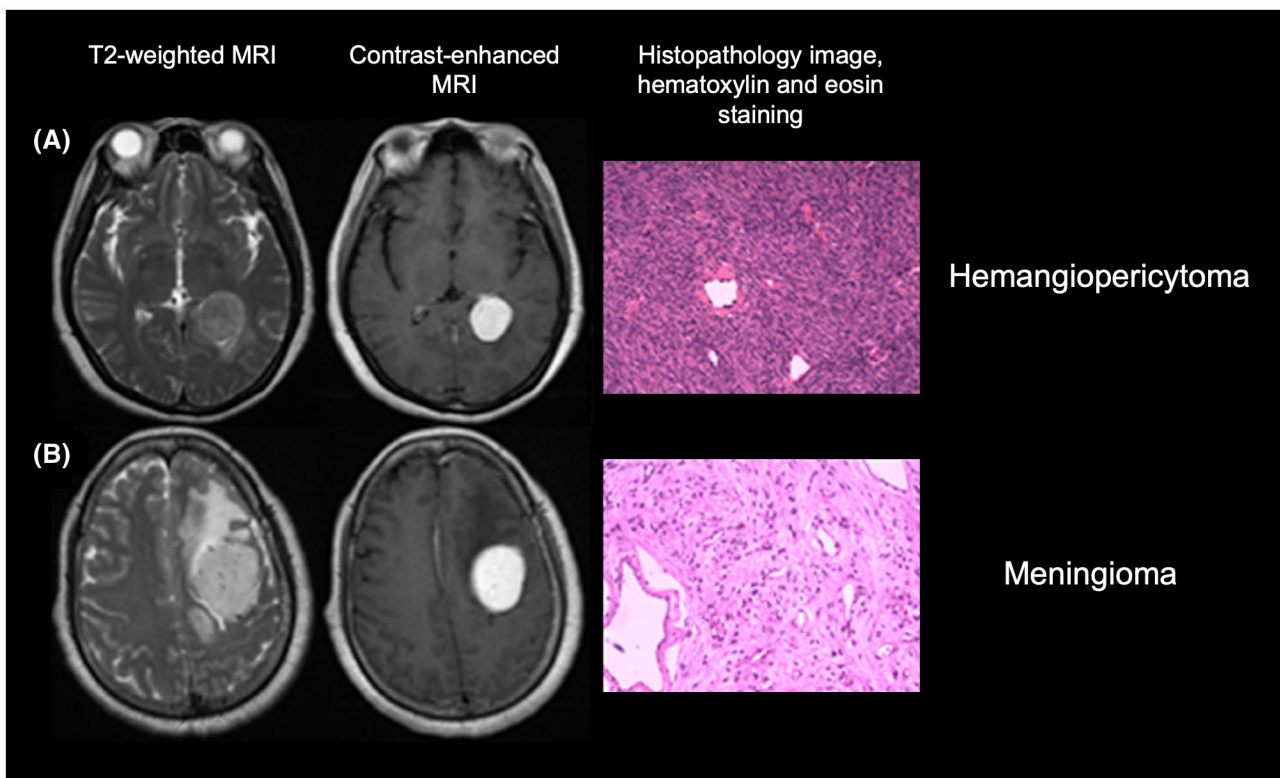


**FIGURE 4** MRI scans and corresponding histopathological images with hematoxylin and eosin staining of two patients diagnosed with a hemangiopericytoma (A) and a meningioma (B). The similar appearance on conventional MRI makes a reliable differential diagnosis difficult. Here, the preoperative extraction of quantitative image features using radiomics provided additional diagnostic information to improve differential diagnosis. Modified from Wei et al. [103], under the terms of the Creative Commons Attribution License (CC-BY, version 4.0)

of hyperperfusion was significantly associated with the presence of a high-grade meningioma (i.e., WHO grade II or III).

A multicenter study included around 400 meningioma patients and suggested that also apparent diffusion coefficients derived from DWI can differentiate WHO grade I meningioma from grade II and III tumors with an accuracy of 73% [57]. Additionally, in that study, the proliferation marker Ki-67 was significantly correlated with ADC derived from DWI. However, it has to be pointed out that predominantly older diffusion and perfusion MRI studies reported no additional value or discrepant results regarding meningioma grading [58–60].

### 4.3 | Meningioma relapse risk stratification

For patient management and treatment decisions, the prediction of an early meningioma relapse, i.e., identifying meningioma patients with increased relapse risk is of great clinical importance. Notably, an earlier diagnosis of meningioma relapse using conventional MR or CT imaging may be impeded by specific tumor locations (e.g., skull base).

A retrospective study in 144 postoperative meningioma patients showed that DWI-derived ADC provides additional information to predict an increased risk for meningioma relapse [61]. Besides other factors, patients with incomplete resection and low ADC had a significantly higher risk of progression or recurrence and may benefit from a more aggressive treatment strategy. Another study investigated the value of ex vivo ultra-high-field proton MRS at 11.4 T of resected tumor tissue to predict aggressive biological behavior in 64 WHO grade I-III meningioma. The absolute concentrations of alanine and creatine, as well as the choline/glutamate and glycine/alanine ratios, were associated with an increased probability of rapid meningioma relapse [62]. By contrast, in vivo MRS has both limited spectral resolution and precision, thereby hampering equivalent analyses, especially of alanine and glutamate.

## 5 | MOST RELEVANT CLINICAL APPLICATIONS FOR PET IMAGING

Several tracers addressing different molecular structures or pathophysiological pathways in meningioma cells are available [33]. Because of the overexpression of SSTRs in meningiomas [32, 63, 64], radiolabeled SSTR ligands are particularly used to visualize meningioma tissue. The SSTR subtype 2 is the most abundant isoform with almost 100% expression in meningiomas [32]. The most commonly applied SSTR ligands for PET imaging in patients with meningioma are DOTATOC and DOTATATE. After labeling with  $^{68}\text{Ga}$ , these ligands are

frequently used as tracers for imaging of neuroendocrine tumors, which likewise express high levels of SSTR [65].  $^{68}\text{Ga}$  has a physical half-life of 68 minutes and can be produced with a  $^{68}\text{Ge}/^{68}\text{Ga}$  generator, enabling in-house production without an on-site cyclotron. PET ligands to SSTR provide high sensitivity with excellent target-to-background contrast due to low uptake in bone and healthy brain tissue [66, 67]. Currently, the number of PET examinations in meningioma patients is steadily increasing.

The L-amino acid transporter system mediates the uptake of radiolabeled amino acids such as [ $^{11}\text{C}$ -methyl]-L-methionine (MET) and O-(2- $^{18}\text{F}$ -fluoroethyl)-L-tyrosine (FET). Increased uptake is seen in slow-growing tumors such as meningiomas [68, 69].

### 5.1 | Meningioma detection

Due to a meningioma localization with low contrast on MRI or CT, e.g., at the skull base with or without osseous involvement of the adjacent skull bone, tumor detection and delineation may be complicated if standard anatomical cross-sectional imaging techniques are applied. Furthermore, meningiomas can be obscured by calcifications or MRI artifacts. The recent body of literature has suggested that SSTR PET adds valuable diagnostic information to MRI or CT to overcome these issues.

A study compared contrast-enhanced MRI with DOTATOC PET in 190 meningioma patients before radiotherapy and reported that all meningiomas were detected by PET, whereas contrast-enhanced MRI detected only 90% of these meningiomas. These findings indicate that the improved sensitivity for DOTATOC PET may identify additional meningiomas even if MRI is negative [66] (Figure 5).

DOTATATE PET studies with histological validation of imaging findings revealed a more precise tumor extent delineation than contrast-enhanced MRI [67, 70]. Furthermore, in meningiomas with complex growth patterns, i.e., involvement of the sagittal or cavernous sinus, the orbita, or infiltration of other osseous structures, PET using DOTATATE and DOTATOC was also reported to provide an improved tumor delineation compared with MRI [71–73]. Another study suggested that DOTATATE PET helps discriminate optic nerve sheath meningiomas from other lesions affecting the optic nerve [74]. Similarly, studies using amino acid PET reported an improved meningioma delineation compared with MRI [68, 75, 76].

Moreover, PET images can be integrated into MR-based neuronavigation systems for image-guided neurosurgery, and the additional information in terms of tumor extent can be used for the intraoperative guidance of resection, e.g., in complex skull base meningiomas.

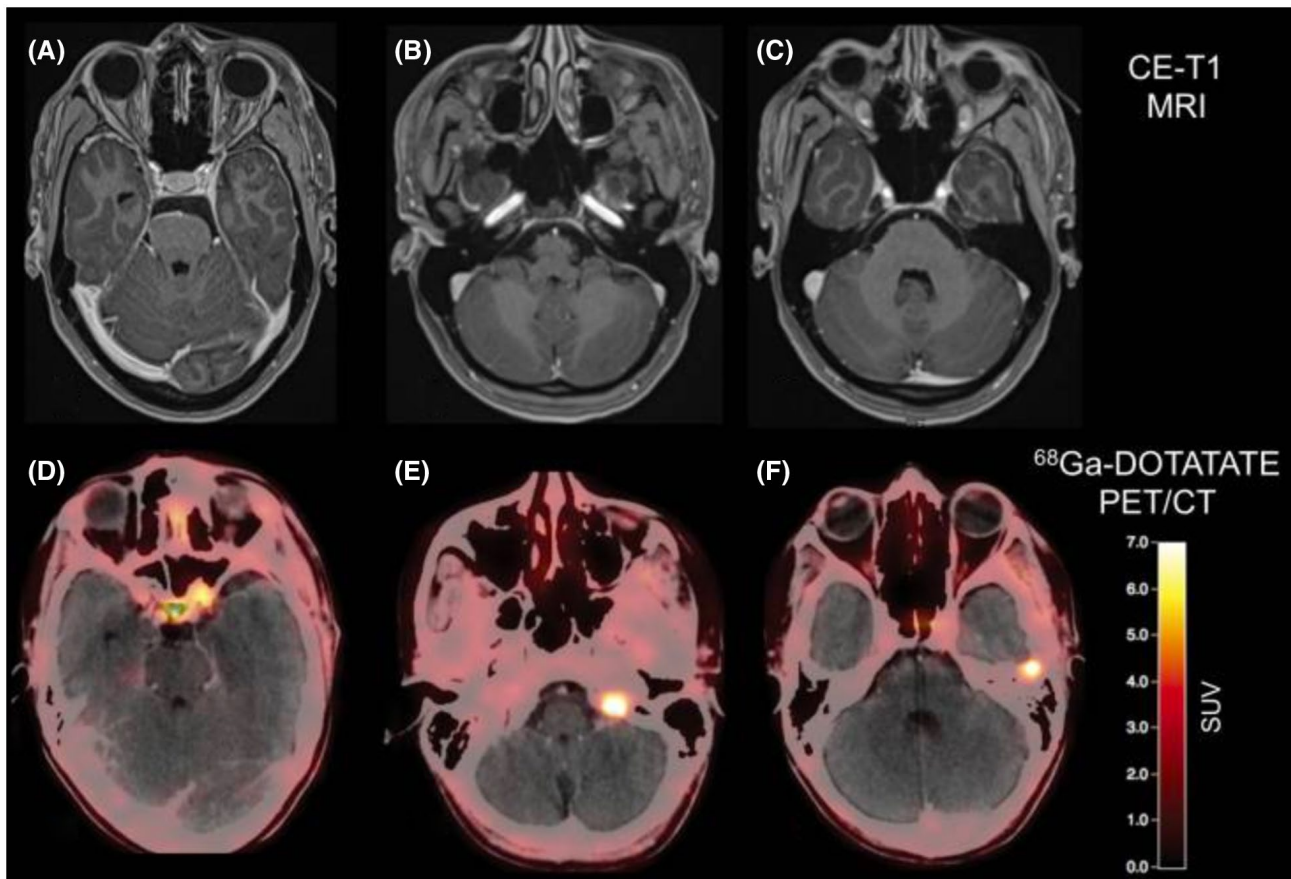


**FIGURE 5** Postoperative contrast-enhanced MRI and DOTATATE PET/CT of a patient after resection of a WHO grade I meningioma show residual tumor located at the left internal carotid artery and a tumor at the tip of the left orbit (A and D). Surprisingly, two additional meningiomas were also visible on the DOTATATE PET/CT (E and F), without corresponding contrast enhancement on MRI (B and C) (reproduced from Galldiks et al. [33], with permission from Oxford University Press)

## 5.2 | Meningioma grading

The uptake of radiolabeled glucose (2- $^{18}\text{F}$ -fluoro-2-deoxy-D-glucose; FDG) correlates significantly with the WHO grade in meningiomas [77, 78], but as a significant limitation, its uptake is not specific for neoplastic tissue and may be increased in inflammatory processes [79]. Regarding PET ligands to SSTR, DOTATATE binding significantly correlates with tumor growth rates in WHO grade I and II meningiomas but is abolished in anaplastic meningiomas [80]. Data on the amino acid tracer MET labeled with  $^{11}\text{C}$  suggest a correlation with proliferative activity in patients with meningioma [81], but are controversial for non-invasive meningioma grading [82, 83]. Furthermore, due to the short half-life of  $^{11}\text{C}$  of 20 minutes, its use is strictly limited to centers with an on-site cyclotron. Preliminary findings revealed that static and dynamic FET parameters might provide additional information for non-invasive grading of meningiomas [69].

## 5.3 | Radiotherapy planning

Target definition plays a crucial role in the planning of high precision radiotherapy using fractionated

radiotherapy or radiosurgery. Despite using the bone window on CT scans, it is challenging to define the infiltration depth in meningiomas with transosseous growth. In these cases, PET imaging may prove helpful. For example, a DOTATATE PET study focusing on transosseous growing meningiomas showed a higher specificity than standard MRI (100% vs. 83%) [70].

Using SSTR ligands, an optimized target volume delineation for fractionated radiation therapy in WHO grade I-III meningiomas could be obtained using DOTATOC PET co-registered to CT and MRI [72]. In all patients, DOTATOC PET provided additional information on the meningioma extent for fractionated stereotactic radiotherapy planning. These results were confirmed by subsequent studies [73, 84–86].

Furthermore, amino acid PET can also be integrated into radiation treatment planning [87] and significantly influence target volume definition in meningioma patients. Astner and colleagues demonstrated that in the vast majority of patients with skull base meningiomas treated with fractionated radiotherapy, MET PET addition changed the target volumes considerably [68]. In that study, MET PET detected additional tumor areas, which were not visualized on conventional CT or MRI,



leading to a target volume enlargement of almost 10%. Furthermore, areas without tumor affection could be excluded from the radiation field, and eloquent structures, such as the optic nerves, the chiasm, or the pituitary gland, could be spared more effectively [68]. Subsequently, it has been demonstrated that the addition of amino acid PET to CT and MRI helps significantly lower the interobserver variability than either modality alone [75, 76].

#### 5.4 | PET during the follow-up of meningioma patients

The recent literature has suggested that SSTR PET can also help differentiate meningioma relapse from post-therapeutic reactive changes, including radiotherapy [45, 66, 67, 88]. For example, Rachinger and colleagues reported a higher specificity for DOTATATE PET compared with standard MRI (74% vs. 65%) [67].

A recent study has suggested that the intraoperative estimation of meningioma extent for resection using Simpson grades is inferior compared with DOTATATE PET [89]. Although 62.5% of patients had a meningioma resection extent according to the Simpson grade I or II, DOTATATE PET revealed tumor remnants [89].

The initial case series also reported that SSTR PET seems to be valuable to detect extracranial metastatic meningioma involving the liver, lung, and bone [90–92].

## 6 | OTHER IMAGING MODALITIES

### 6.1 | Optical imaging

Besides other techniques, Raman spectroscopy is a powerful optical imaging method which allows to analyze the biochemical composition of tissue to differentiate neoplastic from normal tissue. By shining monochromatic laser light onto a sample obtained from brain surgery, this technique detects scattered light to measure the vibrational energy modes of a sample. A small amount of the scattered light shifts in energy from the laser frequency because of interactions between the incident electromagnetic waves and the vibrational energy levels of the molecules in the sample. Plotting the intensity of the shifted light against the frequency creates a Raman spectrum of the sample.

Initial studies suggest that Raman spectroscopy has a high diagnostic accuracy to differentiate between glioma subtypes, brain metastases, and meningioma [93, 94]. Another study highlighted the clinical potential of this technique for the determination of the meningioma grade, i.e., the differentiation between WHO grade I and II [95].

### 6.2 | Intraoperative ultrasound including elastography

For neurosurgical interventions, intraoperative imaging guidance is fundamental to achieve a complete tumor resection and to preserve neurological functions. In this regard, intraoperative ultrasound is a reliable method to obtain real-time information during brain surgery. Furthermore, the biomechanical properties of tissues correlated to histology, and neuropathological findings have also received increased attention in recent years. Ultrasonographic elastography imaging is able to evaluate intraoperatively the elastic properties of tissues such as tissue hardness to distinguish pathologic and healthy areas. An increasing body of literature suggests that elastographic ultrasound patterns may help to identify different brain tumor types, i.e., gliomas, metastases, and meningiomas [96, 97].

## 7 | ARTIFICIAL INTELLIGENCE: RADIOMICS AND RADIOGENOMICS IN PATIENTS WITH MENINGIOMA

A subdiscipline of artificial intelligence dealing with the computation, identification, and extraction of image features for the generation of mathematical models related to the research purpose (e.g., to improve diagnostics) is termed radiomics. Radiomics is usually applied to routinely acquired imaging modalities, thereby allowing additional data analysis at a low cost. Since radiomics features are either mathematically predefined (feature-based radiomics) or generated from the data by training computational models (deep learning-based radiomics), the results are more robust, reliable, and reproducible. Radiogenomics, a subdiscipline of radiomics, aims to correlate radiomics features with molecular markers, genetic mutations, or chromosomal aberrations. Figure 6 shows a representative feature-based radiomics workflow.

### 7.1 | Differentiation between meningiomas and other brain tumors

The differentiation between different brain tumor types based on conventional MRI alone is challenging due to similar imaging findings such as contrast enhancement and perifocal edema (Figure 7). Therefore, artificial intelligence and machine learning methods have been used to differentiate meningiomas from other brain tumor types. The differentiation between meningiomas, gliomas, and tumors of the pituitary gland using modified local binary pattern feature extraction methods was investigated by Kaplan and colleagues [98]. Local binary patterns describe the texture pattern in neuroimages and reflect the correlation among pixels within a local area

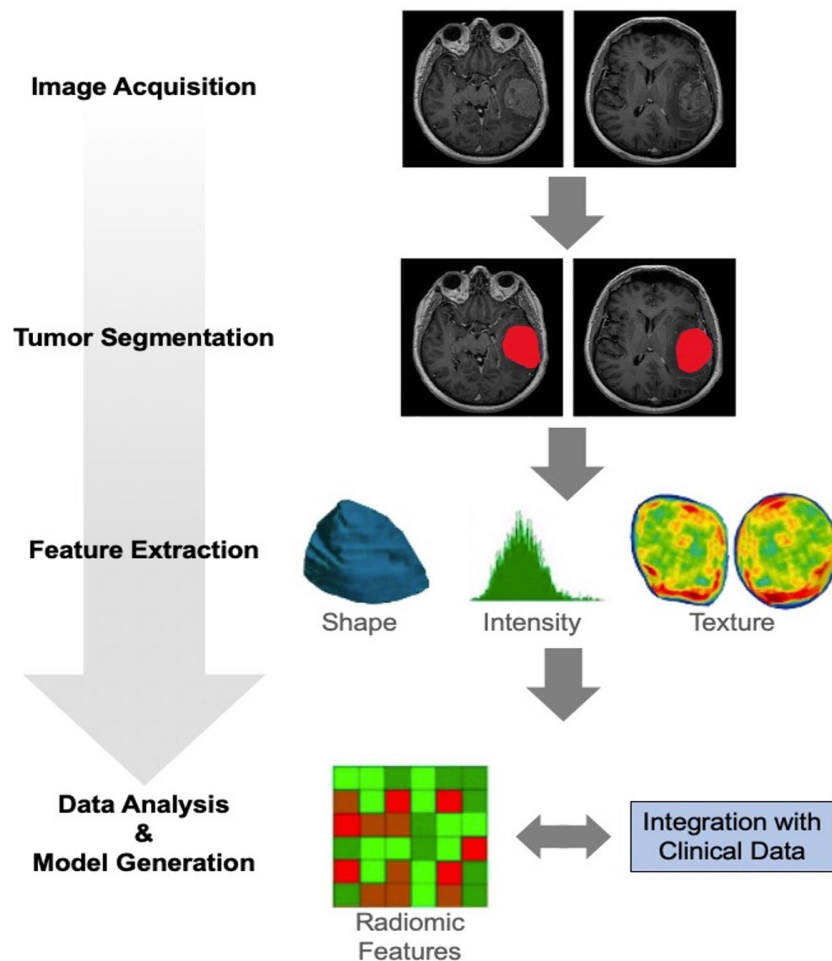


**FIGURE 6** Schematic representation of the radiomics workflow. Following image acquisition, volumes-of-interest within tumor subregions (e.g., contrast enhancement, T2/FLAIR signal hyperintensity) are manually or automatically segmented. Most frequently, shape, intensity, and textural features are calculated. Subsequently, radiomics features are combined with clinical data (e.g., survival times, neuropathology findings), and a mathematical model related to the research question can be generated. Adapted from Gu et al. [130], under the terms of the Creative Commons Attributions License (CC-BY, version 4.0)

[99]. In that study, the dataset consisted of more than 3000 T1-weighted MRI slices from 233 patients. The identified local binary patterns differentiated between meningiomas, gliomas, and pituitary tumors with an accuracy of 96%.

In addition to structural MRI, Shrot and co-workers included perfusion- and diffusion-weighted MRI from 141 patients differentiate between meningioma, glioblastoma, primary central nervous system lymphoma, and brain metastases [100]. The final support vector machine classifier yielded more than 90% classification accuracy for all investigated tumor types. These results are in line with results reported in an earlier study using a similar methodology [101].

Li et al. aimed at a preoperative distinction of malignant hemangiopericytoma from angiomatous meningioma based on structural MRI and DWI [102]. Clinical and textural features were generated, and the performance of the radiomics model was compared with the rating of three experienced neuroradiologists. A support vector machine classifier based on T1-weighted MRI revealed the best diagnostic performance with an area under the curve (AUC) of 0.90, outperforming the neuroradiologists' rating (AUC, 0.73). Similar results could be confirmed by a subsequent study [103].

## 7.2 | Identification of meningioma subtypes

In clinical routine, the mainstay of brain tumor classification, including meningiomas, performed by neuropathologists is based on morphological criteria. Notably, various meningioma subtypes exhibit only minor morphological variations and may challenge meningioma subtyping. To facilitate the neuropathological diagnosis of meningothelial, fibroblastic, transitional, or psammomatous WHO grade I meningioma, Fatima and colleagues [104] developed a hybrid classification technique based on radiomics features of these four subtypes. The selected features were used to train a neural network classifier and yielded an average accuracy of more than 90%.

## 7.3 | Meningioma grading and outcome prediction

For meningioma grading using radiomics features based on structural MRI, radiomics models achieved diagnostic accuracies between 76% and 93% for the differentiation of WHO grade I from WHO grade II or III meningiomas [105–109]. The accuracy could be further increased to

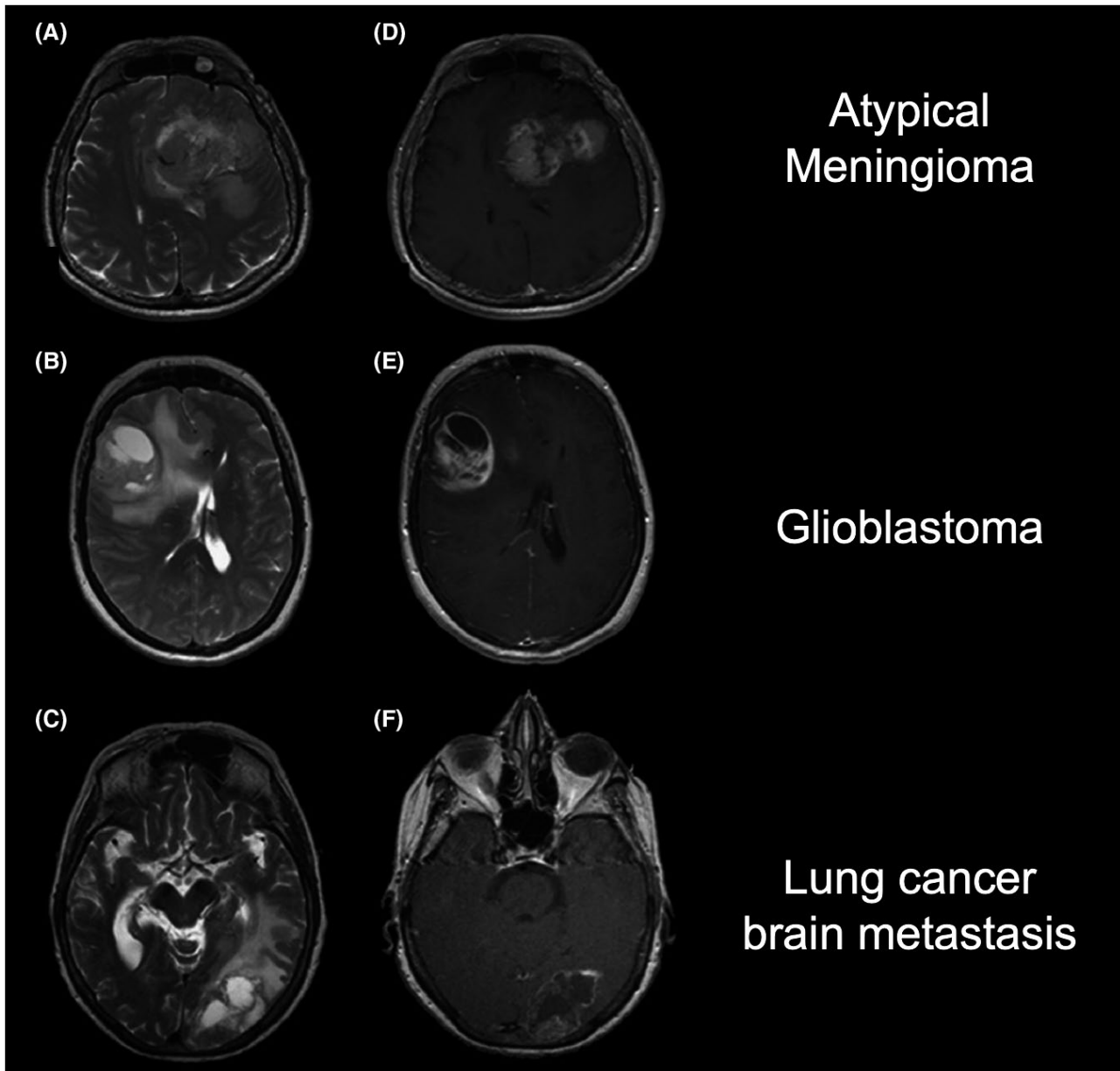


**FIGURE 7** Representative T2-weighted (A–C) and contrast-enhanced T1-weighted MR images (D–F) of an atypical meningioma (top row), a glioblastoma (middle row), and a lung cancer brain metastasis (bottom row). Notably, the similar radiological findings make it difficult to differentiate between these three tumor entities. Here, advanced neuroimaging techniques may provide additional diagnostic information to improve differential diagnosis. Adapted from Svolos et al. [101], with permission from Elsevier

97% by integrating advanced MRI techniques such as DWI to radiomics models [110–116]. Similarly, several studies developed deep learning-based radiomics models based on structural MRI for meningioma grading and achieved diagnostic accuracies between 80 and 83% [117–119]. In addition, Banzato and colleagues [120] developed a deep learning model based on ADC maps derived from DWI that provided a relatively high diagnostic accuracy of 94% for meningioma grading.

Importantly, a recent study has evaluated the robustness of radiomics based on structural MRI data from 25 different scanners acquired using 126 different imaging protocols [121]. Despite that heterogeneity, the developed

deep learning radiomics model yielded a diagnostic accuracy of 74% for meningioma grading, indicating high robustness.

The 2016 edition of the WHO Classification of Tumors of the Central Nervous System has introduced the criterion of brain invasion to diagnose meningiomas of the WHO grade II [122]. Brain invasion is associated with a higher rate of tumor relapse and unfavorable prognosis [123–126]. Consequently, several studies investigated the potential of radiomics for the non-invasive identification of brain invasion [127–129]. For example, in more than 450 patients, Joo and co-workers evaluated structural MRI radiomics features calculated from peritumoral

edema and brain-to-tumor interface [127]. The final model combining the best six radiomics features and peritumoral edema volume yielded an AUC of 0.91 to identify brain invasion.

Initial studies suggest that prognostic models based on clinical parameters and radiologic and radiomic features may preoperatively identify meningiomas at risk for poor outcomes. For example, Morin et al. used preoperative structural and diffusion-weighted MRI scans from 303 patients who underwent resection of 314 meningiomas (57% WHO grade I, 35% grade II, and 8% grade III) to extract 16 radiologic and 172 radiomic features [115]. The colleagues observed that both radiologic and radiomic predictors of adverse meningioma outcomes were significantly associated with molecular markers of aggressive meningioma biology, such as somatic mutation burden, DNA methylation status, and *FOXMI* expression. Furthermore, multivariate analyses revealed that radiomics features obtained from diffusion-weighted MRI were significantly associated with WHO meningioma grades, local failure, and overall survival.

## 8 | CONCLUSIONS AND OUTLOOK

Advanced MRI techniques and PET ligands binding to SSTR can improve the clinical management of patients with meningioma. The translation of these imaging modalities is also of great interest in the light of emerging high-throughput methods such as radiomics. Furthermore, the increasing use of hybrid PET/MRI systems offers an immense research potential for comparative studies under the same (patho-) physiological conditions. Besides, the increasing availability of ultra-high field MRI scanners with higher spatial resolution may help develop novel MRI methods in meningiomas because almost all MRI contrasts benefit from the improved signal-to-noise ratio. Nevertheless, the implementation of advanced MRI and PET methods in clinical routine requires the validation of neuroimaging findings by neuropathology.

Furthermore, various radiomics approaches are promising in terms of the improvement of diagnostics in patients with meningioma. Importantly, the use of advanced imaging techniques may even further improve radiomics models. This may accelerate the translation of decision support systems based on artificial intelligence into daily clinical practice.

### CONFLICT OF INTEREST

Related to the present work, all authors report no conflicts of interest.

### AUTHOR CONTRIBUTIONS

Norbert Galldiks and Philipp Lohmann conceptualized the review article. A review of the literature was performed by Norbert Galldiks, Frank Angenstein, and

Philipp Lohmann. The first draft of the manuscript was written by Norbert Galldiks, Frank Angenstein, and Philipp Lohmann. All other authors commented on previous versions of the manuscript. All authors read and approved the final manuscript.

### DATA AVAILABILITY STATEMENT

Data sharing is not applicable to this article as no new data were created or analyzed in this study.

### ORCID

Norbert Galldiks  <https://orcid.org/0000-0002-2485-1796>

Philipp Lohmann  <https://orcid.org/0000-0002-5360-046X>

### REFERENCES

- Ostrom QT, Cioffi G, Gittleman H, Patil N, Waite K, Kruchko C, et al. CBTRUS statistical report: primary brain and other central nervous system tumors diagnosed in the United States in 2012–2016. *Neuro Oncol.* 2019;21(Suppl 5):v1–100.
- Pieper DR, Al-Mefty O, Hanada Y, Buechner D. Hyperostosis associated with meningioma of the cranial base: secondary changes or tumor invasion. *Neurosurgery.* 1999;44(4):742–46; discussion 6–7.
- Saloner D, Uzelac A, Hetts S, Martin A, Dillon W. Modern meningioma imaging techniques. *J Neurooncol.* 2010;99(3):333–40.
- Aerts HJ, Velazquez ER, Leijenaar RT, Parmar C, Grossmann P, Carvalho S, et al. Decoding tumour phenotype by noninvasive imaging using a quantitative radiomics approach. *Nat Commun.* 2014;5:4006.
- Gillies RJ, Kinahan PE, Hricak H. Radiomics: images are more than pictures, they are data. *Radiology.* 2016;278(2):563–77.
- Lambin P, Leijenaar RTH, Deist TM, Peerlings J, de Jong EEC, van Timmeren J, et al. Radiomics: the bridge between medical imaging and personalized medicine. *Nat Rev Clin Oncol.* 2017;14(12):749–62.
- Lambin P, Rios-Velazquez E, Leijenaar R, Carvalho S, van Stiphout RG, Granton P, et al. Radiomics: extracting more information from medical images using advanced feature analysis. *Eur J Cancer.* 2012;48(4):441–6.
- Sahm F, Schrimpf D, Olar A, Koelsche C, Reuss D, Bissel J, et al. TERT promoter mutations and risk of recurrence in meningioma. *J Natl Cancer Inst.* 2016;108(5):djjv377.
- Wiestler B, Menze B. Deep learning for medical image analysis: a brief introduction. *Neurooncol Adv.* 2020;2(Suppl 4):iv35–41.
- Kalamarides M, Peyre M, Giovannini M. Meningioma mouse models. *J Neurooncol.* 2010;99(3):325–31.
- Mawrin C. Animal models of meningiomas. *Chin Clin Oncol.* 2017;6(Suppl 1):S6.
- Burns SS, Chang LS. Generation of noninvasive, quantifiable, orthotopic animal models for NF2-associated schwannoma and meningioma. *Methods Mol Biol.* 2016;1427:59–72.
- Coombe DR, Nakhoul AM, Stevenson SM, Peroni SE, Sanderson CJ. Expressed luciferase viability assay (ELVA) for the measurement of cell growth and viability. *J Immunol Methods.* 1998;215(1–2):145–50.
- Karimi MA, Lee E, Bachmann MH, Salicioni AM, Behrens EM, Kambayashi T, et al. Measuring cytotoxicity by bioluminescence imaging outperforms the standard chromium-51 release assay. *PLoS One.* 2014;9(2):e89357.
- Kaijzel EL, van der Pluijm G, Löwik CW. Whole-body optical imaging in animal models to assess cancer development and progression. *Clin Cancer Res.* 2007;13(12):3490–7.



16. Baklaushev VP, Kilpeläinen A, Petkov S, Abakumov MA, Grinenko NF, Yusubaliev GM, et al. Luciferase expression allows bioluminescence imaging but imposes limitations on the orthotopic mouse (4T1) model of breast cancer. *Sci Rep*. 2017;7(1):7715.
17. Day C-P, Carter J, Ohler ZW, Bonomi C, El Meskini R, Martin P, et al. “Glowing Head” mice: a genetic tool enabling reliable preclinical image-based evaluation of cancers in immunocompetent allografts. *PLoS One*. 2014;9(11):e109956.
18. Jeon YH, Choi Y, Kang JH, Kim CW, Jeong JM, Lee DS, et al. Immune response to firefly luciferase as a naked DNA. *Cancer Biol Ther*. 2007;6(5):781–6.
19. Baia GS, Dinca EB, Ozawa T, Kimura ET, McDermott MW, James CD, et al. An orthotopic skull base model of malignant meningioma. *Brain Pathol*. 2008;18(2):172–9.
20. Ragel BT, Elam IL, Gillespie DL, Flynn JR, Kelly DA, Mabey D, et al. A novel model of intracranial meningioma in mice using luciferase-expressing meningioma cells. *Laboratory investigation*. *J Neurosurg*. 2008;108(2):304–10.
21. Peyre M, Stemmer-Rachamimov A, Clermont-Taranchon E, Quentin S, El-Taraya N, Walczak C, et al. Meningioma progression in mice triggered by Nf2 and Cdkn2ab inactivation. *Oncogene*. 2013;32(36):4264–72.
22. Chen J, Landegger LD, Sun Y, Ren J, Maimon N, Wu L, et al. A cerebellopontine angle mouse model for the investigation of tumor biology, hearing, and neurological function in NF2-related vestibular schwannoma. *Nat Protoc*. 2019;14(2):541–55.
23. van Furth WR, Laughlin S, Taylor MD, Sahlia B, Mainprize T, Henkelman M, et al. Imaging of murine brain tumors using a 1.5 Tesla clinical MRI system. *Can J Neurol Sci*. 2003;30(4):326–32.
24. Kliese N, Gobrecht P, Pachow D, Andrae N, Wilisch-Neumann A, Kirches E, et al. miRNA-145 is downregulated in atypical and anaplastic meningiomas and negatively regulates motility and proliferation of meningioma cells. *Oncogene*. 2013;32(39):4712–20.
25. Pachow D, Andrae N, Kliese N, Angenstein F, Stork O, Wilisch-Neumann A, et al. mTORC1 inhibitors suppress meningioma growth in mouse models. *Clin Cancer Res*. 2013;19(5):1180–9.
26. Tuchen M, Wilisch-Neumann A, Daniel EA, Baldauf L, Pachow D, Scholz J, et al. Receptor tyrosine kinase inhibition by regorafenib/sorafenib inhibits growth and invasion of meningioma cells. *Eur J Cancer*. 2017;73:9–21.
27. von Spreckelsen N, Waldt N, Poetschke R, Kessele C, Dohmen H, Jiao H-K, et al. KLF4K409Q –mutated skull base meningiomas show enhanced hypoxia response and can be treated by mTORC1 inhibitors. *Acta Neuropathol Commun*. 2020;8(1):41.
28. Wilisch-Neumann A, Kliese N, Pachow D, Schneider T, Warnke JP, Braunsdorf WEK, et al. The integrin inhibitor cilengitide affects meningioma cell motility and invasion. *Clin Cancer Res*. 2013;19(19):5402–12.
29. La Cava F, Fringuello Mingo A, Irrera P, Di Vito A, Cordaro A, Brioschi C, et al. Orthotopic induction of CH157MN convexity and skull base meningiomas into nude mice using stereotactic surgery and MRI characterization. *Animal Model Exp Med*. 2019;2(1):58–63.
30. Kalamarides M, Stemmer-Rachamimov AO, Takahashi M, Han ZY, Chareyre F, Niwa-Kawakita M, et al. Natural history of meningioma development in mice reveals: a synergy of Nf2 and p16(Ink4a) mutations. *Brain Pathol*. 2008;18(1):62–70.
31. Patil R, Ljubimov AV, Gangalum PR, Ding H, Portilla-Arias J, Wagner S, et al. MRI virtual biopsy and treatment of brain metastatic tumors with targeted nanobioconjugates: nanoclinic in the brain. *ACS Nano*. 2015;9(5):5594–608.
32. Dutour A, Kumar U, Panetta R, Ouafik L, Fina F, Sasi R, et al. Expression of somatostatin receptor subtypes in human brain tumors. *Int J Cancer*. 1998;76(5):620–7.
33. Galldiks N, Albert NL, Sommerauer M, Grosu AL, Ganswindt U, Law I, et al. PET imaging in patients with meningioma-report of the RANO/PET Group. *Neuro Oncol*. 2017;19(12):1576–87.
34. Soto-Montenegro ML, Peña-Zalbidea S, Mateos-Pérez JM, Oteo M, Romero E, Morcillo MÁ, et al. Meningiomas: a comparative study of 68Ga-DOTATOC, 68Ga-DOTANOC and 68Ga-DOTATATE for molecular imaging in mice. *PLoS One*. 2014;9(11):e111624.
35. Cal-Gonzalez J, Vaquero JJ, Herraiz JL, Pérez-Liva M, Soto-Montenegro ML, Peña-Zalbidea S, et al. Improving PET quantification of small animal [(68)Ga]DOTA-labeled PET/CT studies by using a CT-based positron range correction. *Mol Imaging Biol*. 2018;20(4):584–93.
36. Ahluwalia MS, Wen PY. Antiangiogenic therapy for patients with glioblastoma: current challenges in imaging and future directions. *Expert Rev Anticancer Ther*. 2011;11(5):653–6.
37. Dhermain FG, Hau P, Lanfermann H, Jacobs AH, van den Bent MJ. Advanced MRI and PET imaging for assessment of treatment response in patients with gliomas. *Lancet Neurol*. 2010;9(9):906–20.
38. Galldiks N, Dunkl V, Stoffels G, Hutterer M, Rapp M, Sabel M, et al. Diagnosis of pseudoprogression in patients with glioblastoma using O-(2-[18F]fluoroethyl)-L-tyrosine PET. *Eur J Nucl Med Mol Imaging*. 2015;42(5):685–95.
39. Kumar AJ, Leeds NE, Fuller GN, Van Tassel P, Maor MH, Sawaya RE, et al. Malignant gliomas: MR imaging spectrum of radiation therapy- and chemotherapy-induced necrosis of the brain after treatment. *Radiology*. 2000;217(2):377–84.
40. Langen KJ, Galldiks N, Hattungen E, Shah NJ. Advances in neuro-oncology imaging. *Nat Rev Neurol*. 2017;13(5):279–89.
41. Galldiks N, Kocher M, Ceccon G, Werner JM, Brunn A, Deckert M, et al. Imaging challenges of immunotherapy and targeted therapy in patients with brain metastases: response, progression, and pseudoprogression. *Neuro Oncol*. 2020;22(1):17–30.
42. Kasten BB, Udayakumar N, Leavenworth JW, Wu AM, Lapi SE, McConathy JE, et al. Current and future imaging methods for evaluating response to immunotherapy in neuro-oncology. *Theranostics*. 2019;9(17):5085–104.
43. Lohmann P, Werner JM, Shah NJ, Fink GR, Langen KJ, Galldiks N. Combined amino acid positron emission tomography and advanced magnetic resonance imaging in glioma patients. *Cancers*. 2019;11(2):153.
44. Huang RY, Bi WL, Griffith B, Kaufmann TJ, la Fougère C, Schmidt NO, et al. Imaging and diagnostic advances for intracranial meningiomas. *Neuro Oncol*. 2019;21(Suppl 1):i44–61.
45. Johnson MD, Powell SZ, Boyer PJ, Weil RJ, Moots PL. Dural lesions mimicking meningiomas. *Hum Pathol*. 2002;33(12):1211–26.
46. Whittle IR, Smith C, Navoo P, Collie D. Meningiomas. *Lancet*. 2004;363(9420):1535–43.
47. Kremer S, Grand S, Remy C, Pasquier B, Benabid AL, Bracard S, et al. Contribution of dynamic contrast MR imaging to the differentiation between dural metastasis and meningioma. *Neuroradiology*. 2004;46(8):642–8.
48. Aronen HJ, Gazit IE, Louis DN, Buchbinder BR, Pardo FS, Weisskoff RM, et al. Cerebral blood volume maps of gliomas: comparison with tumor grade and histologic findings. *Radiology*. 1994;191(1):41–51.
49. Hakyemez B, Erdogan C, Bolca N, Yildirim N, Gokalp G, Parlak M. Evaluation of different cerebral mass lesions by perfusion-weighted MR imaging. *J Magn Reson Imaging*. 2006;24(4):817–24.
50. Kremer S, Grand S, Berger F, Hoffmann D, Pasquier B, Remy C, et al. Dynamic contrast-enhanced MRI: differentiating melanoma and renal carcinoma metastases from high-grade astrocytomas and other metastases. *Neuroradiology*. 2003;45(1):44–9.
51. Kousi E, Tsougos I, Fountas K, Theodorou K, Tsolaki E, Fezoulidis I, et al. Distinct peak at 3.8 ppm observed by 3T MR spectroscopy in meningiomas, while nearly absent in high-grade gliomas and cerebral metastases. *Mol Med Rep*. 2012;5(4):1011–8.
52. Majos C, Alonso J, Aguilera C, Serrallonga M, Coll S, Acebes JJ, et al. Utility of proton MR spectroscopy in the

- diagnosis of radiologically atypical intracranial meningiomas. *Neuroradiology*. 2003;45(3):129–36.
53. Majos C, Cucurella G, Aguilera C, Coll S, Pons LC. Intraventricular meningiomas: MR imaging and MR spectroscopic findings in two cases. *Am J Neuroradiol*. 1999;20(5):882–5.
  54. Lin BJ, Chou KN, Kao HW, Lin C, Tsai WC, Feng SW, et al. Correlation between magnetic resonance imaging grading and pathological grading in meningioma. *J Neurosurg*. 2014;121(5):1201–8.
  55. Ginat DT, Mangla R, Yeane G, Schaefer PW, Wang H. Correlation between dynamic contrast-enhanced perfusion MRI relative cerebral blood volume and vascular endothelial growth factor expression in meningiomas. *Acad Radiol*. 2012;19(8):986–90.
  56. Qiao XJ, Kim HG, Wang DJJ, Salamon N, Linetsky M, Sepahdari A, et al. Application of arterial spin labeling perfusion MRI to differentiate benign from malignant intracranial meningiomas. *Eur J Radiol*. 2017;97:31–6.
  57. Surov A, Ginat DT, Sanverdi E, Lim CCT, Hakyemez B, Yogi A, et al. Use of diffusion weighted imaging in differentiating between malignant and benign meningiomas. A multicenter analysis. *World Neurosurg*. 2016;88:598–602.
  58. Azizyan A, Eboli P, Drazin D, Mirocha J, Maya MM, Bannykh S. Differentiation of benign angiomatous and microcystic meningiomas with extensive peritumoral edema from high grade meningiomas with aid of diffusion weighted MRI. *Biomed Res Int*. 2014;2014:650939.
  59. Sanverdi SE, Ozgen B, Oguz KK, Mut M, Dolgun A, Soylemezoglu F, et al. Is diffusion-weighted imaging useful in grading and differentiating histopathological subtypes of meningiomas? *Eur J Radiol*. 2012;81(9):2389–95.
  60. Zhang H, Rodiger LA, Shen T, Miao J, Oudkerk M. Preoperative subtyping of meningiomas by perfusion MR imaging. *Neuroradiology*. 2008;50(10):835–40.
  61. Hwang WL, Marciscano AE, Niemierko A, Kim DW, Stemmer-Rachamimov AO, Curry WT, et al. Imaging and extent of surgical resection predict risk of meningioma recurrence better than WHO histopathological grade. *Neuro Oncol*. 2016;18(6):863–72.
  62. Pfisterer WK, Nieman RA, Scheck AC, Coons SW, Spetzler RF, Preul MC. Using ex vivo proton magnetic resonance spectroscopy to reveal associations between biochemical and biological features of meningiomas. *Neurosurg Focus*. 2010;28(1):E12.
  63. Menke JR, Raleigh DR, Gown AM, Thomas S, Perry A, Tihan T. Somatostatin receptor 2a is a more sensitive diagnostic marker of meningioma than epithelial membrane antigen. *Acta Neuropathol*. 2015;130(3):441–3.
  64. Reubi JC, Maurer R, Klijn JG, Stefanko SZ, Foekens JA, Blaauw G, et al. High incidence of somatostatin receptors in human meningiomas: biochemical characterization. *J Clin Endocrinol Metab*. 1986;63(2):433–8.
  65. Johnbeck CB, Knigge U, Kjaer A. PET tracers for somatostatin receptor imaging of neuroendocrine tumors: current status and review of the literature. *Future Oncol*. 2014;10(14):2259–77.
  66. Afshar-Oromieh A, Giesel FL, Linhart HG, Haberkorn U, Haufe S, Combs SE, et al. Detection of cranial meningiomas: comparison of (68)Ga-DOTATOC PET/CT and contrast-enhanced MRI. *Eur J Nucl Med Mol Imaging*. 2012;39(9):1409–15.
  67. Rachinger W, Stoecklein VM, Terpolilli NA, Haug AR, Ertl L, Poeschl J, et al. Increased 68Ga-DOTATATE uptake in PET imaging discriminates meningioma and tumor-free tissue. *J Nucl Med*. 2015;56(3):347–53.
  68. Astner ST, Dobrei-Ciuchendea M, Essler M, Bundschuh RA, Sai H, Schwaiger M, et al. Effect of 11C-methionine-positron emission tomography on gross tumor volume delineation in stereotactic radiotherapy of skull base meningiomas. *Int J Radiat Oncol Biol Phys*. 2008;72(4):1161–7.
  69. Cornelius JF, Stoffels G, Filss C, Galldiks N, Slotty P, Kamp M, et al. Uptake and tracer kinetics of O-(2-(18)F-fluoroethyl)-L-tyrosine in meningiomas: preliminary results. *Eur J Nucl Med Mol Imaging*. 2015;42(3):459–67.
  70. Kunz WG, Jungblut LM, Kazmierczak PM, Vettermann FJ, Bollenbacher A, Tonn JC, et al. Improved detection of transosseous meningiomas using (68)Ga-DOTATATE PET/CT Compared with contrast-enhanced MRI. *J Nucl Med*. 2017;58(10):1580–7.
  71. Henze M, Schuhmacher J, Hipp P, Kowalski J, Becker DW, Doll J, et al. PET imaging of somatostatin receptors using [68Ga]DOTA-D-Phe1-Tyr3-octreotide: first results in patients with meningiomas. *J Nucl Med*. 2001;42(7):1053–6.
  72. Milker-Zabel S, Zabel-du Bois A, Henze M, Huber P, Schulz-Ertner D, Hoess A, et al. Improved target volume definition for fractionated stereotactic radiotherapy in patients with intracranial meningiomas by correlation of CT, MRI, and [68Ga]-DOTATOC-PET. *Int J Radiat Oncol Biol Phys*. 2006;65(1):222–7.
  73. Nyuyki F, Plotkin M, Graf R, Michel R, Steffen I, Denecke T, et al. Potential impact of (68)Ga-DOTATOC PET/CT on stereotactic radiotherapy planning of meningiomas. *Eur J Nucl Med Mol Imaging*. 2010;37(2):310–8.
  74. Klingenstein A, Haug AR, Miller C, Hintschich C. Ga-68-DOTATATE PET/CT for discrimination of tumors of the optic pathway. *Orbit*. 2015;34(1):16–22.
  75. Grosu AL, Weber WA, Astner ST, Adam M, Krause BJ, Schwaiger M, et al. 11C-methionine PET improves the target volume delineation of meningiomas treated with stereotactic fractionated radiotherapy. *Int J Radiat Oncol Biol Phys*. 2006;66(2):339–44.
  76. Rutten I, Cabay JE, Withofs N, Lemaire C, Aerts J, Baart V, et al. PET/CT of skull base meningiomas using 2–18F-fluoro-L-tyrosine: initial report. *J Nucl Med*. 2007;48(5):720–5.
  77. Di Chiro G, Hatazawa J, Katz DA, Rizzoli HV, De Michele DJ. Glucose utilization by intracranial meningiomas as an index of tumor aggressivity and probability of recurrence: a PET study. *Radiology*. 1987;164(2):521–6.
  78. Lee JW, Kang KW, Park SH, Lee SM, Paeng JC, Chung JK, et al. 18F-FDG PET in the assessment of tumor grade and prediction of tumor recurrence in intracranial meningioma. *Eur J Nucl Med Mol Imaging*. 2009;36(10):1574–82.
  79. Liu RS, Chang CP, Guo WY, Pan DH, Ho DM, Chang CW, et al. 1–11C-acetate versus 18F-FDG PET in detection of meningioma and monitoring the effect of gamma-knife radiosurgery. *J Nucl Med*. 2010;51(6):883–91.
  80. Sommerauer M, Burkhardt JK, Frontzek K, Rushing E, Buck A, Krayenbuehl N, et al. 68Gallium-DOTATATE PET in meningioma: A reliable predictor of tumor growth rate? *Neuro Oncol*. 2016;18(7):1021–7.
  81. Iuchi T, Iwadate Y, Namba H, Osato K, Saeki N, Yamaura A, et al. Glucose and methionine uptake and proliferative activity in meningiomas. *Neurol Res*. 1999;21(7):640–4.
  82. Arita H, Kinoshita M, Okita Y, Hirayama R, Watabe T, Ishohashi K, et al. Clinical characteristics of meningiomas assessed by (1)(1)C-methionine and (1)(8)F-fluorodeoxyglucose positron-emission tomography. *J Neurooncol*. 2012;107(2):379–86.
  83. Ikeda H, Tsuyuguchi N, Kunihiro N, Ishibashi K, Goto T, Ohata K. Analysis of progression and recurrence of meningioma using (11)C-methionine PET. *Ann Nucl Med*. 2013;27(8):772–80.
  84. Gehler B, Paulsen F, Oksuz MO, Hauser TK, Eschmann SM, Bares R, et al. [68Ga]-DOTATOC-PET/CT for meningioma IMRT treatment planning. *Radiat Oncol*. 2009;4:56.
  85. Graf R, Nyuyki F, Steffen IG, Michel R, Fahdt D, Wust P, et al. Contribution of 68Ga-DOTATOC PET/CT to target volume delineation of skull base meningiomas treated with stereotactic radiation therapy. *Int J Radiat Oncol Biol Phys*. 2013;85(1):68–73.
  86. Mahase SS, Roth O'Brien DA, No D, Roytman M, Skafida ME, Lin E, et al. [68Ga]-DOTATATE PET/MRI as an adjunct imaging modality for radiation treatment planning of meningiomas. *Neuro-Oncology Advances*. 2021;3(1):vdab012.



87. Grosu AL, Lachner R, Wiedenmann N, Stark S, Thamm R, Kneschaurek P, et al. Validation of a method for automatic image fusion (BrainLAB System) of CT data and 11C-methionine-PET data for stereotactic radiotherapy using a LINAC: first clinical experience. *Int J Radiat Oncol Biol Phys.* 2003;56(5):1450–63.
88. Ivanidze J, Roytman M, Lin E, Magge RS, Pisapia DJ, Liechty B, et al. Gallium-68 DOTATATE PET in the evaluation of intracranial meningiomas. *J Neuroimaging.* 2019;29(5):650–6.
89. Ueberschaer M, Vettermann FJ, Forbrig R, Unterrainer M, Siller S, Biczok AM, et al. Simpson grade revisited—intraoperative estimation of the extent of resection in meningiomas versus postoperative somatostatin receptor positron emission tomography/computed tomography and magnetic resonance imaging. *Neurosurgery.* 2020;88(1):140–6.
90. Dalle Ore CL, Magill ST, Yen AJ, Shahin MN, Lee DS, Lucas CG, et al. Meningioma metastases: incidence and proposed screening paradigm. *J Neurosurg.* 2019;132(5):1447–55.
91. Unterrainer M, Ilhan H, Vettermann F, Cyran CC, Tonn JC, Niyazi M, et al. Whole-body staging of metastatic atypical meningioma using 68Ga-DOTATATE PET/CT. *Clin Nucl Med.* 2019;44(3):227–8.
92. Villanueva-Meyer JE, Magill ST, Lee JC, Umetsu SE, Flavell RR. Detection of metastatic meningioma to the liver using 68Ga-DOTA-octreotate PET/CT. *Clin Nucl Med.* 2018;43(9):e338–e40.
93. Aguiar RP, Falcao ET, Pasqualucci CA, Silveira L Jr. Use of Raman spectroscopy to evaluate the biochemical composition of normal and tumoral human brain tissues for diagnosis. *Lasers Med Sci.* 2020. <https://doi.org/10.1007/s10103-020-03173-1>.
94. Galli R, Meinhardt M, Koch E, Schackert G, Steiner G, Kirsch M, et al. Rapid label-free analysis of brain tumor biopsies by near infrared Raman and fluorescence spectroscopy—A study of 209 patients. *Front Oncol.* 2019;9:1165.
95. Morais CLM, Lilo T, Ashton KM, Davis C, Dawson TP, Gurusinghe N, et al. Determination of meningioma brain tumour grades using Raman microspectroscopy imaging. *Analyst.* 2019;144(23):7024–31.
96. Cepeda S, Barrena C, Arrese I, Fernandez-Perez G, Sarabia R. Intraoperative ultrasonographic elastography: a semi-quantitative analysis of brain tumor elasticity patterns and peritumoral region. *World Neurosurg.* 2020;135:e258–70.
97. Della Pepa GM, Menna G, Stifano V, Pezzullo AM, Auricchio AM, Rapisarda A, et al. Predicting meningioma consistency and brain-meningioma interface with intraoperative strain ultrasound elastography: a novel application to guide surgical strategy. *Neurosurg Focus.* 2021;50(1):E15.
98. Kaplan K, Kaya Y, Kuncan M, Ertunç HM. Brain tumor classification using modified local binary patterns (LBP) feature extraction methods. *Med Hypotheses.* 2020;139:109696.
99. Ojala T, Pietikainen M, Maenpaa T. Multiresolution gray-scale and rotation invariant texture classification with local binary patterns. *IEEE Trans Pattern Anal Mach Intell.* 2002;24(7):971–87.
100. Shrot S, Salhov M, Dvorski N, Konen E, Averbuch A, Hoffmann C. Application of MR morphologic, diffusion tensor, and perfusion imaging in the classification of brain tumors using machine learning scheme. *Neuroradiology.* 2019;61(7):757–65.
101. Svolos P, Tsolaki E, Theodorou K, Fountas K, Kapsalaki E, Fezoulidis I, et al. Classification methods for the differentiation of atypical meningiomas using diffusion and perfusion techniques at 3-T MRI. *Clin Imaging.* 2013;37(5):856–64.
102. Li X, Lu Y, Xiong J, Wang D, She D, Kuai X, et al. Presurgical differentiation between malignant haemangiopericytoma and angiomatous meningioma by a radiomics approach based on texture analysis. *J Neuroradiol.* 2019;46(5):281–7.
103. Wei J, Li L, Han Y, Gu D, Chen Q, Wang J, et al. Accurate preoperative distinction of intracranial hemangiopericytoma from meningioma using a multihabitat and multisequence-based radiomics diagnostic technique. *Front Oncol.* 2020;10:534.
104. Fatima K, Arooj A, Majeed H. A new texture and shape based technique for improving meningioma classification. *Microsc Res Tech.* 2014;77(11):862–73.
105. Chen C, Guo X, Wang J, Guo W, Ma X, Xu J. The diagnostic value of radiomics-based machine learning in predicting the grade of meningiomas using conventional magnetic resonance imaging: a preliminary study. *Front Oncol.* 2019;9:1338.
106. Chu H, Lin X, He J, Pang P, Fan B, Lei P, et al. Value of MRI radiomics based on enhanced T1WI images in prediction of meningiomas grade. *Acad Radiol.* 2021;28(5):687–93.
107. Hale AT, Stonko DP, Wang L, Strother MK, Chambless LB. Machine learning analyses can differentiate meningioma grade by features on magnetic resonance imaging. *Neurosurg Focus.* 2018;45(5):E4.
108. Han Y, Wang T, Wu P, Zhang H, Chen H, Yang C. Meningiomas: Preoperative predictive histopathological grading based on radiomics of MRI. *Magn Reson Imaging.* 2021;77:36–43.
109. Yan PF, Yan L, Hu TT, Xiao DD, Zhang Z, Zhao HY, et al. The Potential value of preoperative MRI texture and shape analysis in grading meningiomas: a preliminary investigation. *Transl Oncol.* 2017;10(4):570–7.
110. Hamerla G, Meyer HJ, Schob S, Ginat DT, Altman A, Lim T, et al. Comparison of machine learning classifiers for differentiation of grade 1 from higher gradings in meningioma: a multi-center radiomics study. *Magn Reson Imaging.* 2019;63:244–9.
111. Hu J, Zhao Y, Li M, Liu J, Wang F, Weng Q, et al. Machine learning-based radiomics analysis in predicting the meningioma grade using multiparametric MRI. *Eur J Radiol.* 2020;131:109251.
112. Ke C, Chen H, Lv X, Li H, Zhang Y, Chen M, et al. Differentiation between benign and nonbenign meningiomas by using texture analysis from multiparametric MRI. *J Magn Reson Imaging.* 2020;51(6):1810–20.
113. Laukamp KR, Shakirin G, Baeßler B, Thiele F, Zopf D, Große Hokamp N, et al. Accuracy of radiomics-based feature analysis on multiparametric magnetic resonance images for noninvasive meningioma grading. *World Neurosurg.* 2019;132:e366–e90.
114. Lu Y, Liu L, Luan S, Xiong J, Geng D, Yin B. The diagnostic value of texture analysis in predicting WHO grades of meningiomas based on ADC maps: an attempt using decision tree and decision forest. *Eur Radiol.* 2019;29(3):1318–28.
115. Morin O, Chen WC, Nassiri F, Susko M, Magill ST, Vasudevan HN, et al. Integrated models incorporating radiologic and radiomic features predict meningioma grade, local failure, and overall survival. *Neurooncol Adv.* 2019;1(1):vdz011.
116. Park YW, Oh J, You SC, Han K, Ahn SS, Choi YS, et al. Radiomics and machine learning may accurately predict the grade and histological subtype in meningiomas using conventional and diffusion tensor imaging. *Eur Radiol.* 2019;29(8):4068–76.
117. Zhang H, Mo J, Jiang H, Li Z, Hu W, Zhang C, et al. Deep learning model for the automated detection and histopathological prediction of meningioma. *Neuroinformatics.* 2021;19(3):393–402.
118. Zhu H, Fang Q, He H, Hu J, Jiang D, Xu K. Automatic prediction of meningioma grade image based on data amplification and improved convolutional neural network. *Comput Math Methods Med.* 2019;2019:7289273.
119. Zhu Y, Man C, Gong L, Dong D, Yu X, Wang S, et al. A deep learning radiomics model for preoperative grading in meningioma. *Eur J Radiol.* 2019;116:128–34.
120. Banzato T, Causin F, Della Puppa A, Cester G, Mazzai L, Zotti A. Accuracy of deep learning to differentiate the histopathological grading of meningiomas on MR images: a preliminary study. *J Magn Reson Imaging.* 2019;50(4):1152–9.
121. Wodzinski M, Banzato T, Atzori M, Andrearczyk V, Cid YD, Muller H. Training deep neural networks for small and highly heterogeneous MRI datasets for cancer grading. *Annu Int Conf IEEE Eng Med Biol Soc.* 2020;2020:1758–61.
122. Louis DN, Perry A, Reifenberger G, von Deimling A, Figarella-Branger D, Cavenee WK, et al. The 2016 World Health

- Organization classification of tumors of the central nervous system: a summary. *Acta Neuropathol.* 2016;131(6):803–20.
123. Brokinkel B, Hess K, Mawrin C. Brain invasion in meningiomas—clinical considerations and impact of neuropathological evaluation: a systematic review. *Neuro Oncol.* 2017;19(10):1298–307.
124. Ho DM, Hsu CY, Ting LT, Chiang H. Histopathology and MIB-1 labeling index predicted recurrence of meningiomas: a proposal of diagnostic criteria for patients with atypical meningioma. *Cancer.* 2002;94(5):1538–47.
125. Nowosielski M, Galldiks N, Iglseider S, Kickingereder P, von Deimling A, Bendszus M, et al. Diagnostic challenges in meningioma. *Neuro Oncol.* 2017;19(12):1588–98.
126. Vranic A, Popovic M, Cör A, Prestor B, Pizem J. Mitotic count, brain invasion, and location are independent predictors of recurrence-free survival in primary atypical and malignant meningiomas: a study of 86 patients. *Neurosurgery.* 2010;67(4):1124–32.
127. Joo L, Park JE, Park SY, Nam SJ, Kim YH, Kim JH, et al. Extensive peritumoral edema and brain-to-tumor interface MR imaging features enable prediction of brain invasion in meningioma: development and validation. *Neuro Oncol.* 2021;23(2):324–33.
128. Kandemirli SG, Chopra S, Priya S, Ward C, Locke T, Soni N, et al. Presurgical detection of brain invasion status in meningiomas based on first-order histogram based texture analysis of contrast enhanced imaging. *Clin Neurol Neurosurg.* 2020;198:106205.
129. Zhang J, Yao K, Liu P, Liu Z, Han T, Zhao Z, et al. A radiomics model for preoperative prediction of brain invasion in meningioma non-invasively based on MRI: a multicentre study. *EBioMedicine.* 2020;58:102933.
130. Gu H, Zhang X, di Russo P, Zhao X, Xu T. The current state of radiomics for meningiomas: promises and challenges. *Front Oncol.* 2020;10:567736.

**How to cite this article:** Galldiks N, Angenstein F, Werner J-M, Bauer EK, Gutsche R, Fink GR, et al. Use of advanced neuroimaging and artificial intelligence in meningiomas. *Brain Pathol.* 2022;32:e13015. <https://doi.org/10.1111/bpa.13015>